

Interface Engineering in Nanostructured Nickel Phosphide Catalyst for Efficient and Stable Water Oxidation

Junyuan Xu,[†] Xian-Kui Wei,[‡] José Diogo Costa,[†] José Luis Lado,[§] Bryan Owens-Baird,^{||} Liliana P. L. Gonçalves,[†] Soraia P. S. Fernandes,[†] Marc Heggen,[‡] Dmitri Y. Petrovykh,[†] Rafal E. Dunin-Borkowski,[‡] Kirill Kovnir,^{||} and Yury V. Kolen'ko^{*,†}

[†] International Iberian Nanotechnology Laboratory, Braga 4715-330, Portugal.

[‡] Ernst Ruska-Centre for Microscopy and Spectroscopy with Electrons and Peter Grünberg Institute, Forschungszentrum Jülich GmbH, 52425 Jülich, Germany.

[§] QuantaLab, International Iberian Nanotechnology Laboratory, Braga 4715-330, Portugal.

^{||} Department of Chemistry, University of California, Davis, Davis, CA 95616, USA.

*yury.kolenko@inl.int

COMPUTATIONAL METHODOLOGY

Structure relaxation of pure Ni₂P and its 33% Mg-doped analogue was performed with density functional theory (DFT) using the Quantum Espresso simulation package^{14a} with projector augmented wave pseudopotentials^{14b} and the Perdew–Burke–Ernzerhof exchange correlation functional.^{14c} The density of states (DOS) and electron localization function (ELF) were calculated with previously optimized structures using the all-electron linearized augmented plane wave package Elk^{14d} in a *k*-mesh with $10 \times 10 \times 10$ points. The projection of the density of states (PDOS) was averaged over different atoms of the same type.

A comparison of diagrams of the elemental PDOS (Figures S2c and S2d) shows the broadening effect of Mg doping on the Ni 3d orbitals, resulting in a merging of the three original spectral peaks into one and enhancing the DOS around the Fermi energy (Figures S2g and S2h). We then analyzed the influence of chemical bonding in pure and doped Ni₂P using ELF analysis. ELF slices along (001) show that Mg substitution changes the ELF distribution around the P atoms (Figures S2e and S2f).

CHEMICALS

Carbon paper (Toray Paper 120), Mg and Ni sputtering targets (Materion), red P powder (98.9%, Alfa Aesar), MgO (nanopowder, 99+%, Alfa Aesar), NiO (nanopowder, 99.8%, Sigma-Aldrich), RuO₂ (anhydrous, 99.9%, Alfa Aesar), IrO₂ (99%, Alfa Aesar), KOH (≥85%, Sigma-Aldrich) and Pt wire (99.9%, Sigma-Aldrich) were used as received. Ultrapure water (18.2 MΩ cm⁻², TOC < 3 p.p.b.) was generated using a Milli-Q Advantage A10 system (Millipore). Solid state reactions were carried out using Ni powder (99.996%, Alfa Aesar), red P powder (99%, Alfa Aesar), and Mg turnings (99.98%, Alfa Aesar) as received.

SYNTHESIS AND CHARACTERIZATION OF THE CATALYSTS

Since CP is hydrophobic, it was first subjected to an O₂ plasma treatment for 5 min (Harrick Plasma), in order to increase its wetting properties in aqueous media. Next, a 200 nm layer of Mg and subsequently a 200 nm layer of Ni were sputtered onto both sides of the CP using a multitarget ultrahigh vacuum sputtering system (Kenosistec). The composite CP was then subjected to an alloying

heat treatment at 600 °C for 2 h under Ar, followed by gas transport phosphorization at 500 °C for 6 h under Ar using 0.3 g of red P powder per 2.4 × 10 cm² of the CP specimen. The control CP-supported pristine Ni₂P catalyst was prepared in the same fashion, but without deposition of a Mg layer. The as-synthesized electrodes are denoted as-grown (AG) and Ni₂P for convenience. The resulting mass densities of the Mg-modified Ni₂P and control pure Ni₂P catalysts were gravimetrically (Cubis MCM36, Sartorius) estimated to be 1.33 mg cm⁻² and 1.16 mg cm⁻², respectively. The specific surface area of the CP-supported Mg-modified Ni₂P and control pure Ni₂P were measured to be about 72 m² g⁻¹ and 67 m² g⁻¹, respectively (Autosorb iQ₂, Quantachrome).

The catalysts were analyzed using powder X-ray diffraction (XRD, X'Pert PRO, PANalytical), scanning electron microscopy (SEM, JSM-7400F, JEOL) and high-angle annular dark-field scanning transmission electron microscopy (HAADF-STEM, Titan 80-200 Chemi-STEM, FEI) equipped with a Super-X energy dispersive X-ray spectrometer (EDX), as well as inductively coupled plasma – optical emission spectroscopy (ICP-OES, ICPE-9000, Shimadzu). According to the ICP-OES results, the molar ratio between Mg and Ni was estimated to be 0.24 in Mg-modified Ni₂P catalyst. Unit cell refinements were performed with WinCSD¹⁵ using a Ge internal standard. The X-ray photoelectron spectroscopy (XPS) measurements were performed using a monochromated microfocused Al K_α X-ray source that defined an analysis spot of ca. 900 × 600 μm². All spectra were acquired in normal emission with an effective analyzer collection angle of ≈ 30°. Aliphatic C 1s peak was observed at binding energy (BE) of 284.5 ± 0.3 eV without the use of charge neutralization, indicating the absence of overall sample charging. The peaks were broadened, however, for all the elements by about 2× compared to the values for similar systems, suggesting heterogeneity of electrical conductivity across the sample.

Solid state synthesis of Mg-doped Ni₂P was carried out through direct reaction of the elements. Two samples were prepared with a Ni:Mg:P ratio of 1.6:0.4:1 and loaded into carbonized silica ampoules in air, evacuated and flame-sealed. The first ampoule was heated to 850 °C over 10 h, annealed at this temperature for 96 h, cooled to 600 °C over 24 h, and cooled to room temperature in the turned-off furnace. The second ampoule was heated to 500 °C over 10 h, annealed at this temperature for 96 h, and cooled to room temperature in the turned-off furnace. The samples were

analyzed by XRD using a Rigaku Miniflex 600 diffractometer employing Cu- $K\alpha$ radiation.

ELECTROCHEMICAL EXPERIMENTS

Electrochemical water oxidation experiments were carried out at room temperature in a three electrode assembly using a geometrically well-defined piece of C paper with the supported catalyst as the working electrode, a Pt wire as the counter electrode and a saturated calomel electrode (SCE) as the reference electrode. The electrolyte was aq. 1 M KOH. For comparison, the electrocatalytic performance of commercial high surface area RuO₂, IrO₂, NiO and MgO materials supported on a carbon paper (loading: 1.3 mg cm⁻²) was also evaluated. The measurements were controlled with a potentiostat/galvanostat (VMP-3, Biologic) while carrying out linear sweep voltammetry (LSV) at 5 mV s⁻¹ in the range 1.2 to 1.8 V_{RHE}, applying 85% internal-resistance (*iR*) compensation. The *iR* values were measured by single-point high-frequency impedance measurements. The durability test was performed using galvanostatic electrolysis at a fixed current density of 10 mA cm⁻² while monitoring the variation of overpotential for 200 h.

O₂ TOFs per mass loading of Mg-modified Ni₂P catalyst were estimated according to the equation $\text{TOF} (\text{O}_2 \text{ s}^{-1}) = (jA)/(4Fn)$, where *j* is the current density at a given overpotential (A cm⁻²), *A* is the surface area of the electrode (1.0 cm²), *F* is the Faraday constant (96500 C mol⁻¹), and *n* is the mole number of the metal in the electrode (mol). The *n* was determined from the equation $n = 1.33 \cdot 10^{-3} \text{ g cm}^{-2} * 1.0 \text{ cm}^2 / \text{metal molar mass}$. We assumed that all of the metal ions were catalytically active, although in reality most likely that some metal sites are inaccessible for water oxidation, and thus the calculated TOF represents the lowest estimated value.

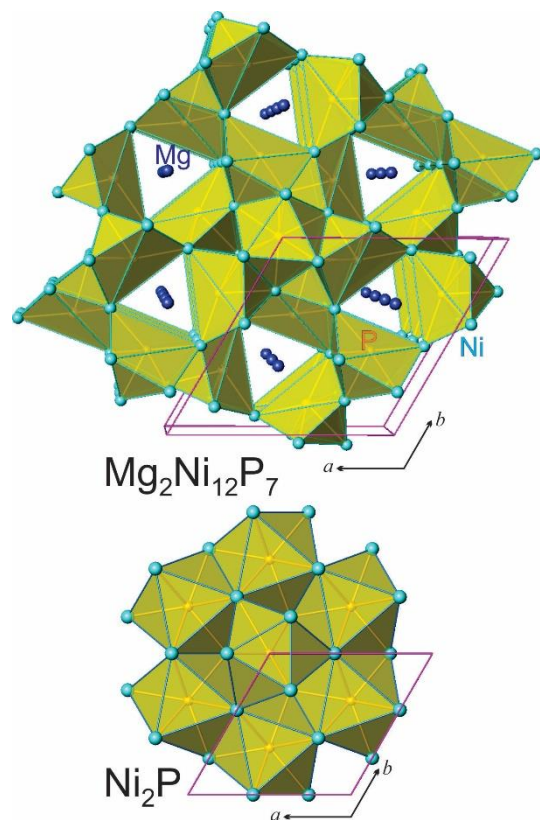


Figure S1. Polyhedral representations of the crystal structures of Mg₂Ni₁₂P₇ and Ni₂P viewed along the [001] direction. Unit cells are shown with purple lines. Mg: blue; Ni: cyan; P: yellow. In the crystal structure of Mg₂Ni₁₂P₇ (~[Mg_{0.14}Ni_{0.86}]₂P), one third of the P atoms are coordinated by 9 Ni atoms, which is similar to the coordination of P atoms in Ni₂P. The other two thirds of the P atoms are coordinated in a similar manner, but by 7 Ni + 2 Mg atoms.

FIGURES

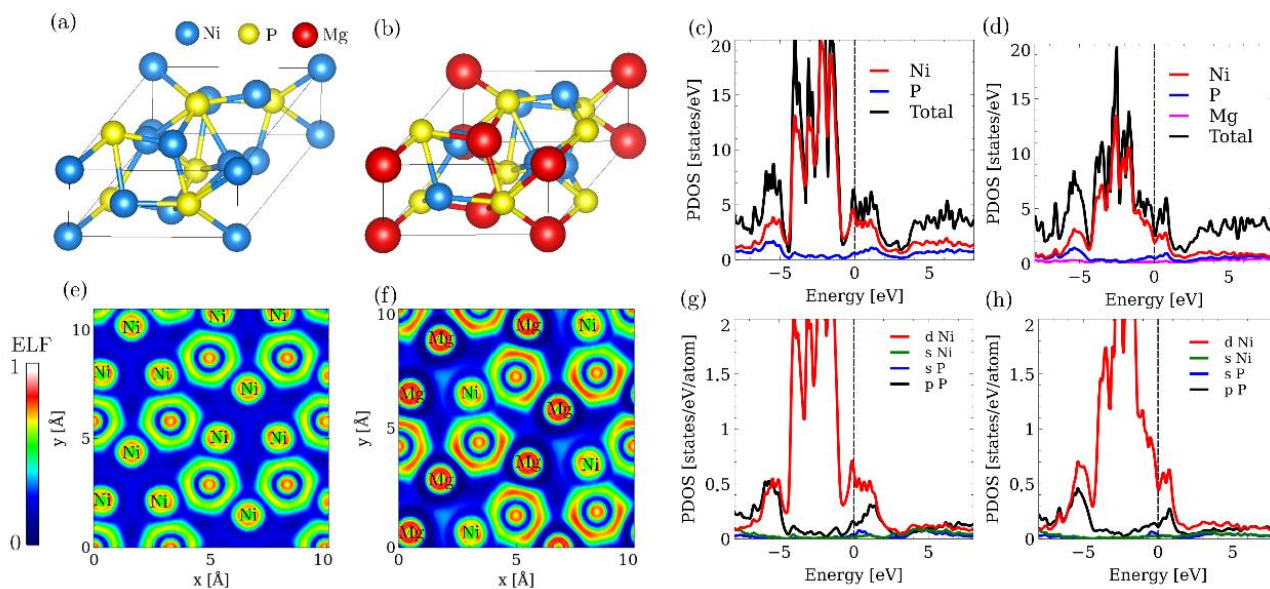


Figure S2. Atomic structure, PDOS diagrams, and ELF slices along the (001) plane of pure Ni_2P (a, e, c) and its relaxed 33% Mg-doped $\text{Ni}_4\text{Mg}_2\text{P}_3$ analog (b, f, d). Comparisons of the partial contributions of Ni 3d, Ni 4s, P 3s, and P 3p are shown in (g) for pure Ni_2P and in (h) for 33% Mg-doped Ni_2P .

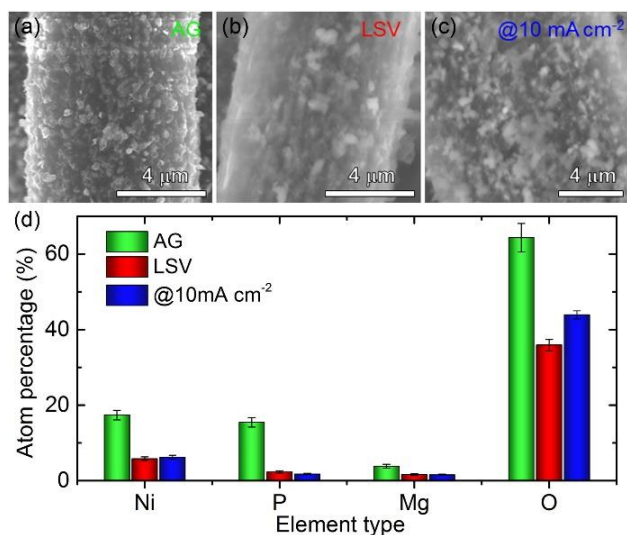


Figure S3. High magnification SEM images of (a) the as-grown (AG), (b) the LSV- and (c) the durability-tested ($@10 \text{ mA cm}^{-2}$) Mg-modified Ni_2P catalyst. (d) Comparison of the mass percentage of elements before and after the electrochemical tests.